PACIFIC EARTHQUAKE ENGINEERING
RESEARCH CENTER

Two-Dimensional Debris-Fluid-Structure Interaction with the Particle Finite Element Method

Minjie Zhu
Michael H. Scott

School of Civil and Construction Engineering
Oregon State University, Corvallis, OR

PEER Report No. 2024/04

Pacific Earthquake Engineering Research Center
Headquarters at the University of California, Berkeley
April 2024

PEER 2024/04
April 2024

Two-Dimensional Debris-Fluid-Structure Interaction with the Particle Finite Element Method

Minjie Zhu
Michael H. Scott

School of Civil and Construction Engineering
Oregon State University, Corvallis, OR

PEER Report No. 2024/04
Pacific Earthquake Engineering Research Center
Headquarters, University of California, Berkeley
April 2024

ABSTRACT

In addition to tsunami wave loading, tsunami-driven debris can cause significant damage to coastal infrastructure and critical bridge lifelines. Using numerical simulations to predict loads imparted by debris on structures is necessary to supplement the limited number of physical experiments of in-water debris loading. To supplement SPH-FEM (Smoothed Particle Hydrodynamics-Finite Element Method) simulations described in a companion PEER report, fluid-structure-debris simulations using the Particle Finite Element Method (PFEM) show the debris modeling capabilities in OpenSees. A new contact element simulates solid to solid interaction with the PFEM. Two-dimensional simulations are compared to physical experiments conducted in the Oregon State University Large Wave Flume by other researchers and the formulations are extended to three-dimensional analysis. Computational times are reported to compare the PFEM simulations with other numerical methods of modeling fluid-structure interaction (FSI) with debris. The FSI and debris simulation capabilities complement the widely used structural and geotechnical earthquake simulation capabilities of OpenSees and establish the foundation for multi-hazard earthquake and tsunami simulation to include debris.

Keywords: Fluid-structure interaction, OpenSees, finite element method, debris, tsunami

ACKNOWLEDGMENTS and DISCLAIMER

The research summarized in this report was made possible through a subaward from the University of Nevada, Reno (UNR) to Oregon State University (OSU). The authors thank Denis Istrati, Anis Hasanpour, and Ian Buckle from UNR for their support and for providing detailed information on the SPH models that allowed OSU to validate the OpenSeesPy PFEM implementations and modeling results summarized in this report.

This work was supported by the State of California through the Transportation Systems Research Program of the Pacific Earthquake Engineering Research (PEER) Center. Any opinions, findings, conclusions or recommendations expressed in this material are those of the authors and do not necessarily reflect the view of the funding agency, Pacific Earthquake Engineering Research (PEER) Center, or the Regents of the University of California.

CONTENTS

LIST OF FIGURES

1 Introduction

Background for research on tsunami-driven debris is followed by a brief introduction to the governing equations and formulation of the Particle Finite Element Method for fluid-structure-debris interaction.

1.1 BACKGROUND AND MOTIVATION

Tsunami induced loading has been responsible for failure and collapse of coastal infrastructure in recent events such as the 2004 Indian Ocean Tsunami, and the 2011 Tohoku Tsunami. In the Indian Ocean tsunami in Sri Lanka and Thailand, debris impact was one of the main causes of structural damage, Rossetto et al. (2007). Field surveys of 2011 Japan Tohoku Tsunami have shown that in the port of Sendai-Shiogama, 60% of containers stored in the terminal were transported by tsunami waves over the harbor apron, Goseberg et al. (2017). Due to the container weight and dimensions, transport becomes a significant threat to coastal infrastructure.

In addition to hazard quantification, current structural engineering research has focused on other aspects of tsunami loading on structures, not just debris. The horizontal and vertical hydrodynamic forces induced by steady flows and wave impact forces at the leading edge of the arriving water mass are also important forces to consider, Yeh et al. (2014). Different types of forces can be identified, such as hydrostatic forces determined by the flow depth, hydrodynamic forces determined by flow depth and velocity, and debris impact forces determined by debris velocity, mass, and stiffness, Charvet et al. (2014). The development of new ASCE *Minimum Design Loads for Building and Other Structures* ASCE (2022) and bridge design specifications, Lynett et al. (2021), reflects the growing emphasis of designing coastal infrastructure to resist tsunami load effects.

Experiments have been conducted to investigate the impact of moving debris on structures Stolle et al. (2020); Riggs et al. (2013); Aghl et al. (2014); Ko et al. (2015). The experiments contain in-air and in-water tests with single and multiple objects, and investigated different debris sizes and geometry and impact angles. In addition to experiments, analytical studies and numerical simulations help quantify debris impact forces on structures. Since many uncertain factors affect debris loading, particularly velocity and flow conditions, experiments are difficult to repeat and numerical simulations can help guide the design of meaningful experiments. Analytical relationships between debris mass and impact velocity and impact loads imparted by individual objects on rigid structures have been proposed, Haehnel and Daly (2004); Como and Mahmoud (2013); Paczkowski et al. (2012). Impact and debris loading have also been simulated using various numerical methods, Nistor et al. (2017). One-way solid-fluid coupling moves solids through the fluid and obtains the solid response without affecting the fluid. Different methods are used to track and model the solids, such as discrete element method (DEM), smoothed-particle hydrodynamics (SPH), and moving particle simulations (MPS). These models assume a rigid structure, which is not sufficient when engineering demand parameters such as deformations and local forces are required for structural design and assessment.

1.2 PARTICLE FINITE ELEMENT METHOD (PFEM)

The Particle Finite Element Method (PFEM) assumes a Lagrangian formulation for both structural and fluid domains, Oñate et al. (2011); Zhu and Scott (2014), and provides a good alternative for two-way modeling of debris, fluid, and structure interaction. For PFEM, the governing equation for the conservation of momentum at all points in the structural domain is

$$\rho \dot{v}_i = \frac{\partial \sigma_{ij}}{\partial x_j} + \rho b_i \tag{1.1}$$

where x_i, u_i and v_i are the coordinates, displacements, and velocities, respectively, of the material point and ρ and b_i are the material density and body acceleration. The constitutive equation is a general nonlinear function of the displacements and velocities

$$\sigma_{ij} = \sigma_{ij}(u_i, v_i) \tag{1.2}$$

where σ_{ij} is the Cauchy stress tensor. Any constitutive model can be used in this formulation, making it straightforward to incorporate hysteresis and viscosity in the constitutive response Simo and Hughes (1998).

The fluid is assumed to be incompressible Newtonian flow, for which conservation of momentum is identical to that for the structural domain in Eq. (1.1). The conservation of mass equation enforces incompressibility of the fluid

$$\frac{\partial v_i}{\partial x_i} = 0 \tag{1.3}$$

and the Cauchy stress tensor is decomposed into spherical and deviatoric parts

$$\sigma_{ij} = s_{ij} - p\delta_{ij} \tag{1.4}$$

with the Kronecker delta, δ_{ij}, and the average stress (pressure), $p = \sigma_{ii}/3$, which is positive for compression. The deviatoric stress, s_{ij}, is defined in terms of the strain rate by

$$s_{ij} = 2\mu \left(\varepsilon_{ij} - \frac{1}{3}\varepsilon_v \delta_{ij} \right) \tag{1.5}$$

where μ is the viscosity, ε_{ij} is the strain rate, and ε_v is the divergence of the velocity field, which may be non-zero for compressible or quasi-incompressible flows

$$\varepsilon_{ij} = \frac{1}{2}\left(\frac{\partial v_i}{\partial x_j} + \frac{\partial v_j}{\partial x_i} \right), \quad \varepsilon_v = \varepsilon_{ii} = \frac{\partial v_i}{\partial x_i} \tag{1.6}$$

Conditions for the entire boundary of the structural and fluid domains can be split into the natural boundary conditions on the surface, Γ_t,

$$\sigma_{ij} n_j = t_i \tag{1.7}$$

where t_i is the surface traction and n_j is the unit vector normal to the boundary surface and the essential boundary condition on the surface, Γ_v,

$$x_i = x_i^p \tag{1.8}$$

where x_i^p is the prescribed coordinates. All points on the surface of both the structural and fluid domains satisfy either natural or essential boundary conditions.

In the classic PFEM, the fluid and structure are combined in the moving mesh of both domains. Although the moving mesh makes the interaction straightforward to implement, it has the limitation of small time steps and mesh distortion. A fixed fluid mesh was proposed Becker et al. (2015) to allow for larger time steps and to alleviate mesh distortion. A background mesh approach has been proposed Zhu and Scott (2022) for more computationally efficient interaction between a fixed fluid mesh and a moving structural mesh. Both debris and structures are modeled as moving structural meshes, the fluid-debris and fluid-structure interactions are included in the interaction between the fixed fluid mesh and the moving structural mesh. The debris-structure interaction is handled through contact elements between them. Since the background mesh approach keeps track of locations of all structures and debris on the background grid, it is straightforward to detect the contact and to create contact elements between debris and structures.

All implementation and simulations presented in this work utilize the OpenSees software framework (McKenna et al. (2010)) and the OpenSeesPy Python module (Zhu et al. (2018)).

2 Two-Dimensional Modeling

A debris impact experiment (Ko et al. (2015)) was conducted at the Large Wave Flume (LWF) O. H. Hinsdale Wave Research Laboratory (HWRL) at Oregon State University (OSU). As shown in Fig. 2.1, the LWF is 110 m long, 3.7 m wide, and 4.6 m deep. The piston wavemaker, located at x = 0, has a maximum stroke length of 4 m and a maximum speed of 4 m/s. Two wave gauges were placed at x = 24.87 m and x = 35.83 m to record the wave heights and velocities with acoustic doppler velocimeters (ADVs).

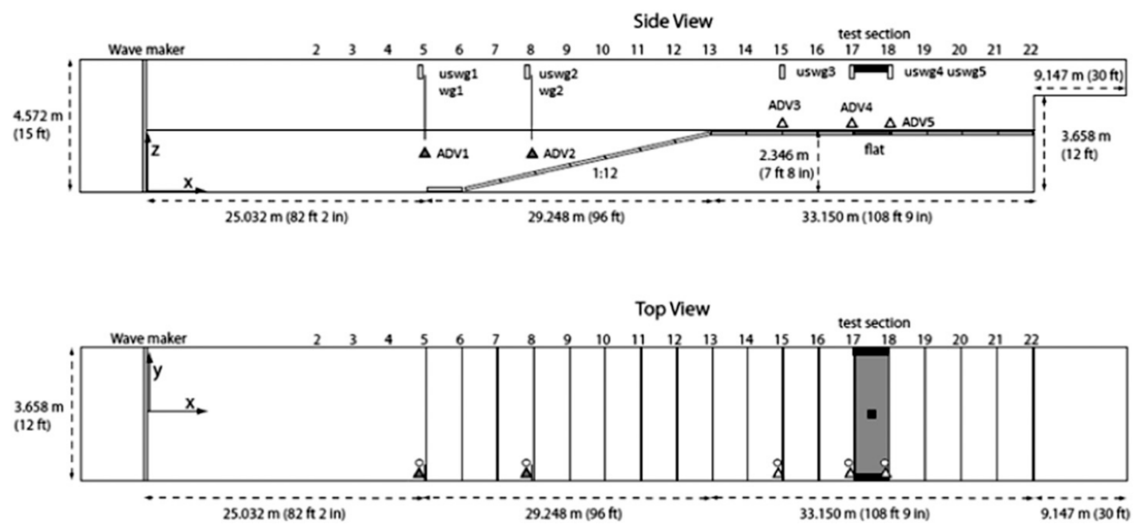

Figure 2.1: Dimensions of OSU Large Wave Flume.

2.1 NUMERICAL MODEL OF WAVE FLUME

The OpenSeesPy PFEM model contains 143,874 fluid elements, 143,648 fluid velocity degrees of freedom (DOFs), 74,116 fluid pressure DOFs, 1,518,361 fluid particles, and 72 elements for debris as shown in Fig. 2.2. The water is modeled as fluid particles in red which move on the background mesh. The debris and the column are modeled with beam-column elements on the right side of the flume. The wavemaker is modeled as beam-column elements with prescribed displacements and velocities.

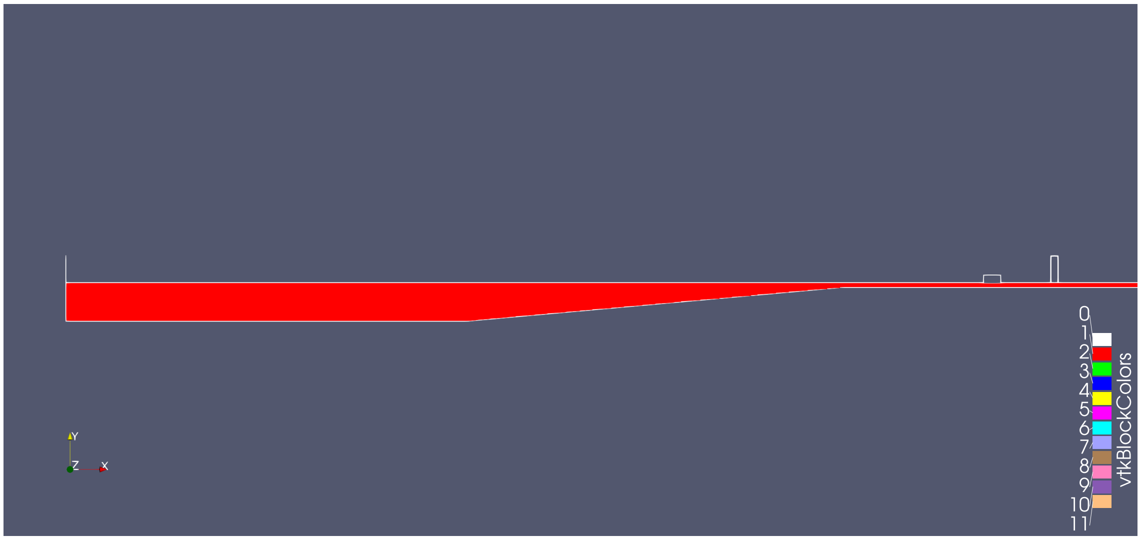

Figure 2.2: Numerical model of wave flume and wave maker in PFEM.

The numerical model for SPH consisted of 14,571 shell elements and 1,193,075 particles with particle size of 1 cm as shown in Hasanpour et al. (2021, 2022); Hasanpour (2023); Hasanpour et al. (2023).

The motion of the wavemaker is shown in Fig. 2.3, where the displacement was increased from 0 m to 4 m in 60 seconds. The fitted curves for displacement and velocity are applied to the nodes of the wavemaker beam-column elements to simulate the wavemaker motion in the analysis. In OpenSeesPy, the prescribed displacements and velocities are imposed in the horizontal direction.

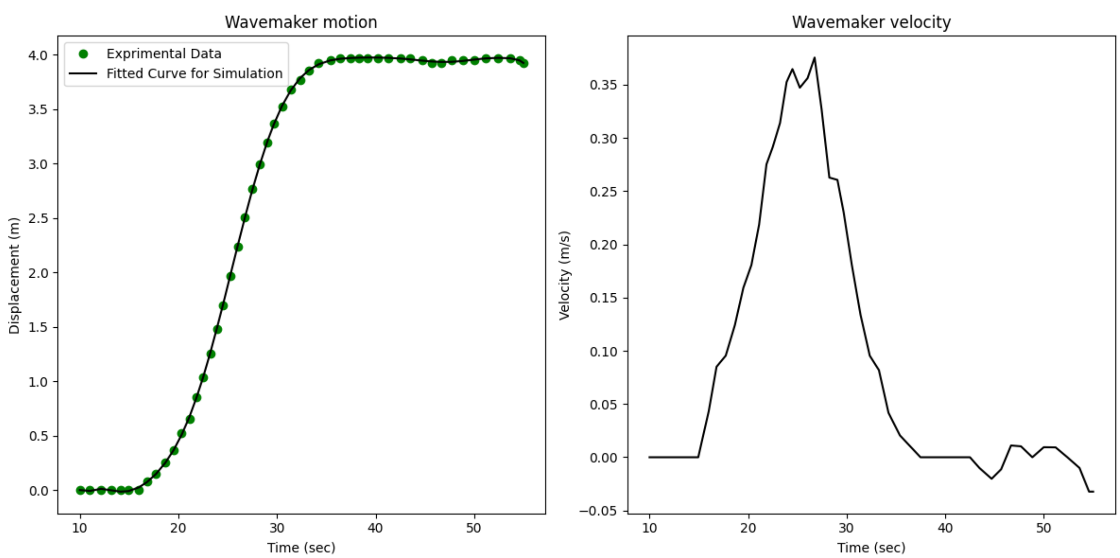

Figure 2.3: The wavemaker motion in experiment and its fitted curve for simulation.

2.2 SIMULATION OF WAVE PROPAGATION

The analysis was first run *without* debris in order to verify the free surface height and wave velocities at the two wave gauges locations. As shown in Fig. 2.4, the PFEM results from OpenSeesPy show very close response histories compared with the experiment Ko et al. (2015) and the SPH results Hasanpour et al. (2021) for both wave heights and velocities.

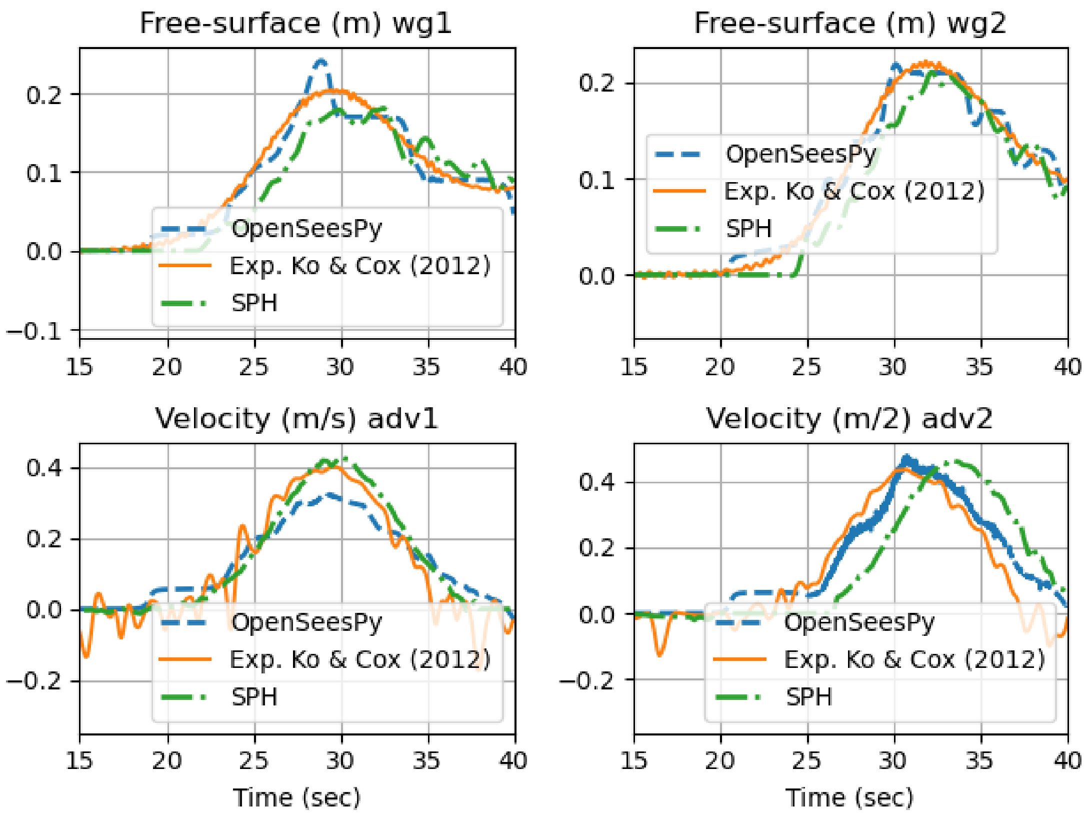

Figure 2.4: Comparison of free surface and wave velocities at wave gauges 1 and 2 between experimental results, SPH, and the PFEM in OpenSeesPy.

2.3 SIMULATION OF TSUNAMI DRIVEN DEBRIS

In the experiment, the debris is an aluminum 1:5-scale model of a 1.22 x 0.49 x 0.58 m shipping container. In the analysis, the debris is modeled as 2D corotational elastic beam-column elements. The model allows the large displacements of the debris. Since the debris is rigid in the experiment, a high elasticity is applied in the simulation and no deformation will be observed. As shown in Fig. 2.5, the debris is initially placed 3.5 m to the left of the column and right above the water surface.

To match the conditions of the experiment, the following model adjustments and checks were made:

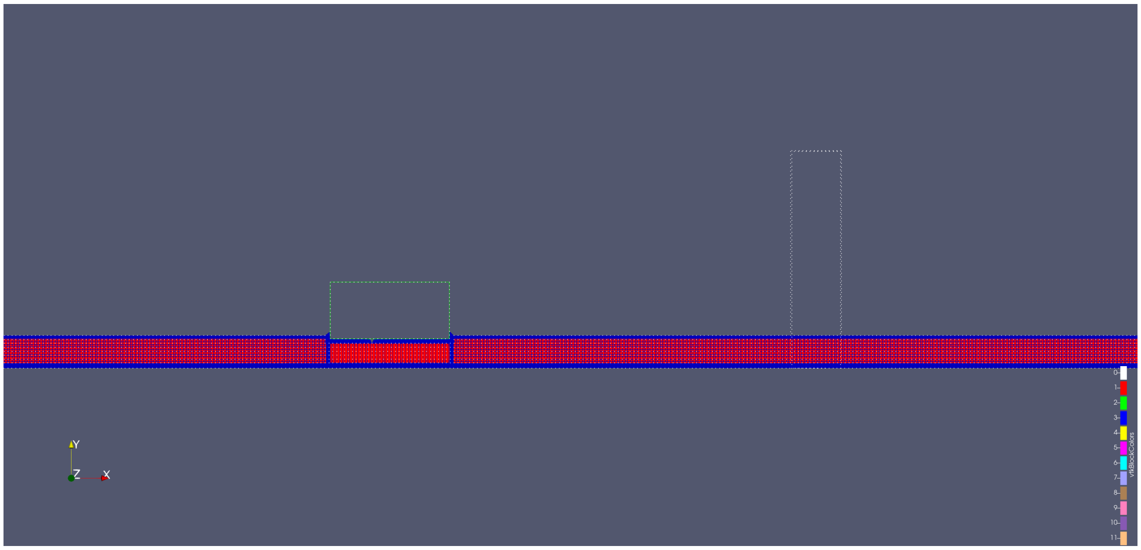

Figure 2.5: Initial location of debris relative to column in OpenSeesPy simulation of debris impact.

- According to the experiment, the debris stays in its initial location until the wave comes. However, the PFEM numerical simulations, as well as simulations performed using SPH Hasanpour (2023), show the debris will move a small distance to the left before the wave arrives and will change the time of debris impact on the column accordingly. In the physical experiment, the debris was also kept in place by a vertical beam setup. Therefore, this motion could be physical or numerical due to the finite mesh size of the water which forms gaps between water particles when the wave was propagating. These gaps are much smaller in the physical experiment but relatively large and comparable to the mesh size of the problem.

  Therefore, a temporary fix condition is applied in the x-direction at two left corners of the debris. Once the waves arrives, the temporary fix conditions are removed, allowing the debris to move freely. Although we can reduce the mesh size to make the numerical simulation closer to the physics, a temporary fixity solves the problem with minimum efforts.

- The draft of the debris measured in the experiment was 0.09 m. The OpenSeesPy PFEM simulation matches the experimentally observed value as shown in Fig. 2.6. This check ensures the body forces applied to the debris model match the weight of debris from the experiment and that the 2D simulation replicates 3D draft effects.

- When the wave hit the column in the experiment, fluid will flow around the base of the obstacle. However, the numerical simulation is 2D, and all fluid will impact, or dam up behind the obstacle. To circumvent this issue of 2D simulation, fluid-structure interaction (FSI) between the column and the fluid was turned off, but the column can still interact with the debris. The implementation of PFEM in OpenSeesPy was changed to select structures to be able to interact with the fluid so that the column can interact with the debris but not the fluid. This change also improves the impact forces.

  As shown in Fig. 2.7, contact elements, which simulate solid-solid interaction, are formed

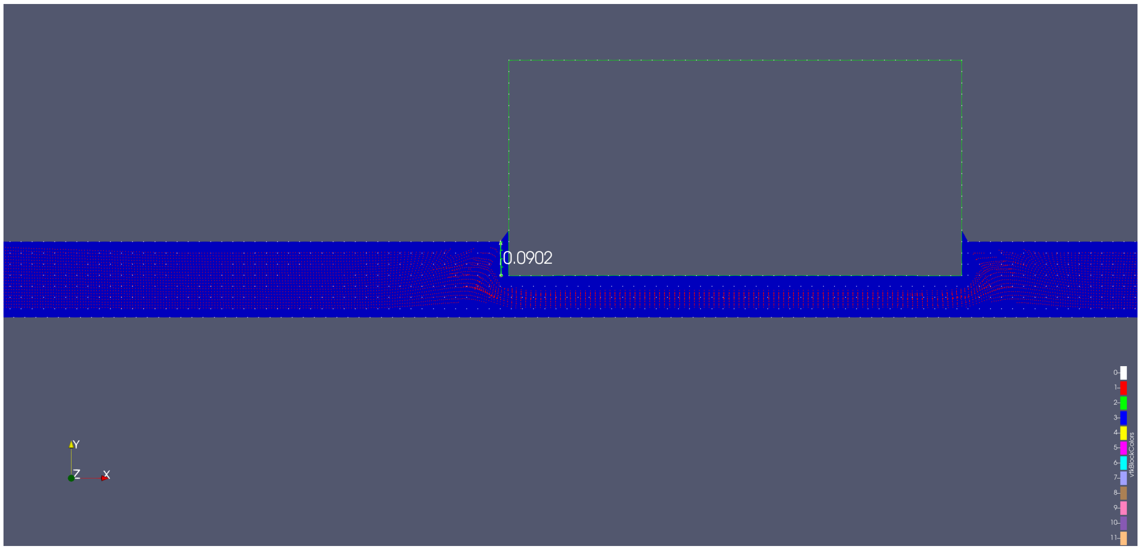

Figure 2.6: Initial draft of the debris.

between the debris and the column. The figure shows the water freely moving through the column without blockage.

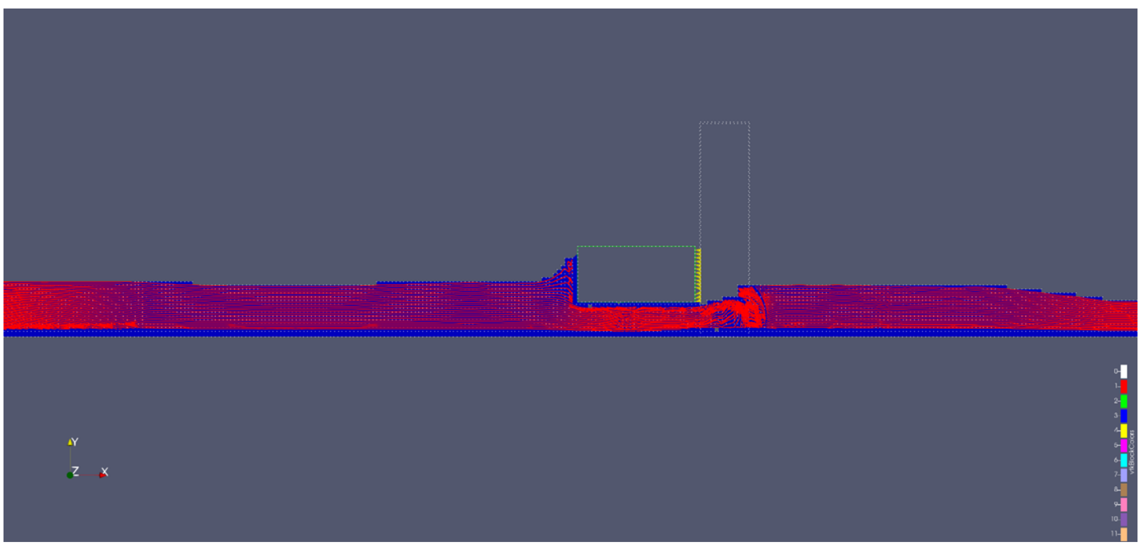

Figure 2.7: The interaction between column and debris and non-interaction between column and water.

- As indicated in the Ko and Cox experiment, a guide wire was used in order to prevent the yaw. Pitching and off-center impact was observed in some cases but were discarded because they were not considered "good" trials for the experiment. It is straightforward to simulate the guided debris in OpenSeesPy by fixing the rotational degrees of freedom of the debris nodes. As shown in Fig. 2.7, even at the time of impact with the column, the debris keeps its original orientation, i.e., the debris translates and impacts the column without rotating.

2.3.1 Compare debris velocity with experiments and SPH

The comparison of debris velocity history with Hasanpour (2023) using SPH is shown in Fig. 2.8. The speed of four corners of the debris are recorded and compared with the experimental data. Though the debris velocity was estimated visually based on videos recordings in the experiment, a good match can be seen for the time that debris starts moving, the impact time, and peak velocity.

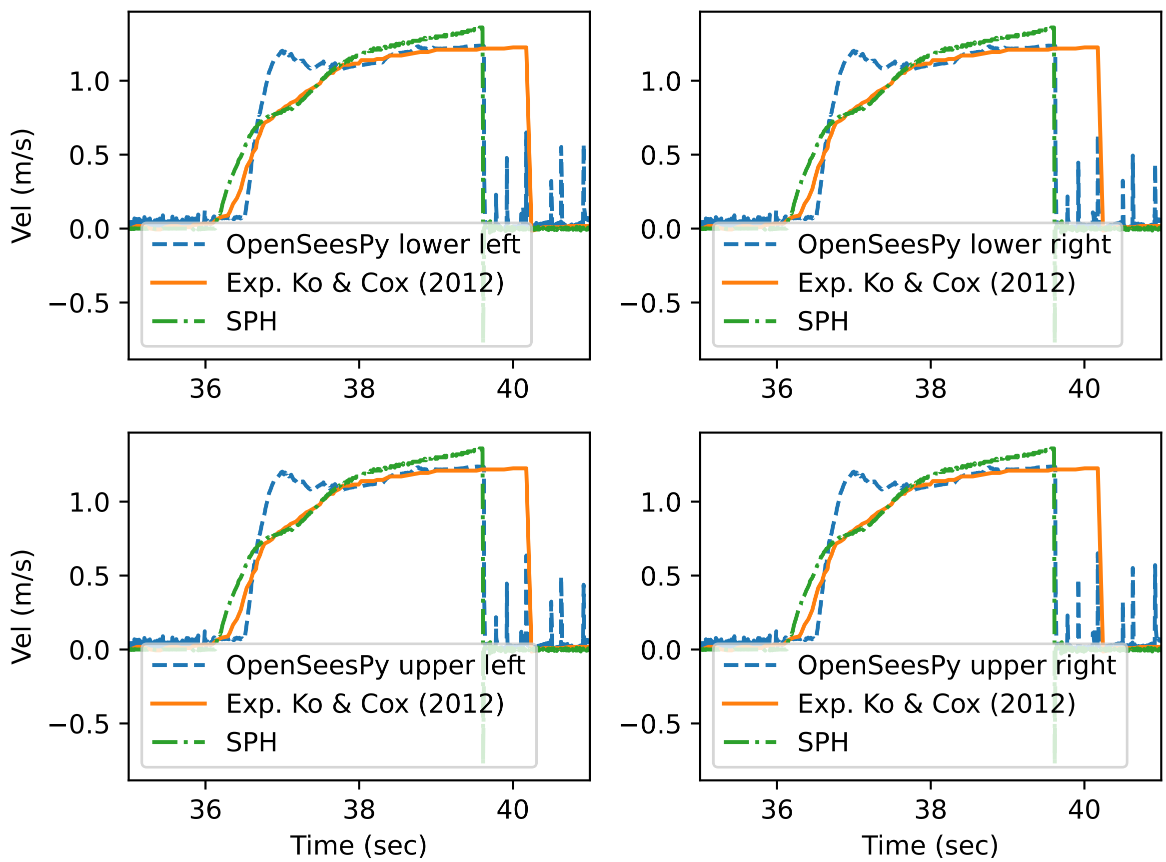

Figure 2.8: Comparison of debris velocities between PFEM OpenSeesPy simulations, experimental results, and SPH.

2.3.2 Compare impact forces with experiments and SPH

The impact forces of the debris on the column are shown in Fig. 2.9. Similar to the SPH-FEM simulations in Hasanpour et al. (2021, 2023), large spikes are observed in the response history of impact force. These spikes can be attributed to the high stiffness assigned to the debris model in order to simulate rigid behavior. In addition, the impact force is a highly random process. However, it is promising that the two simulation approaches show good agreement on the peak force, which is about 30% difference and is often the only response quantity of interest for impact loading.

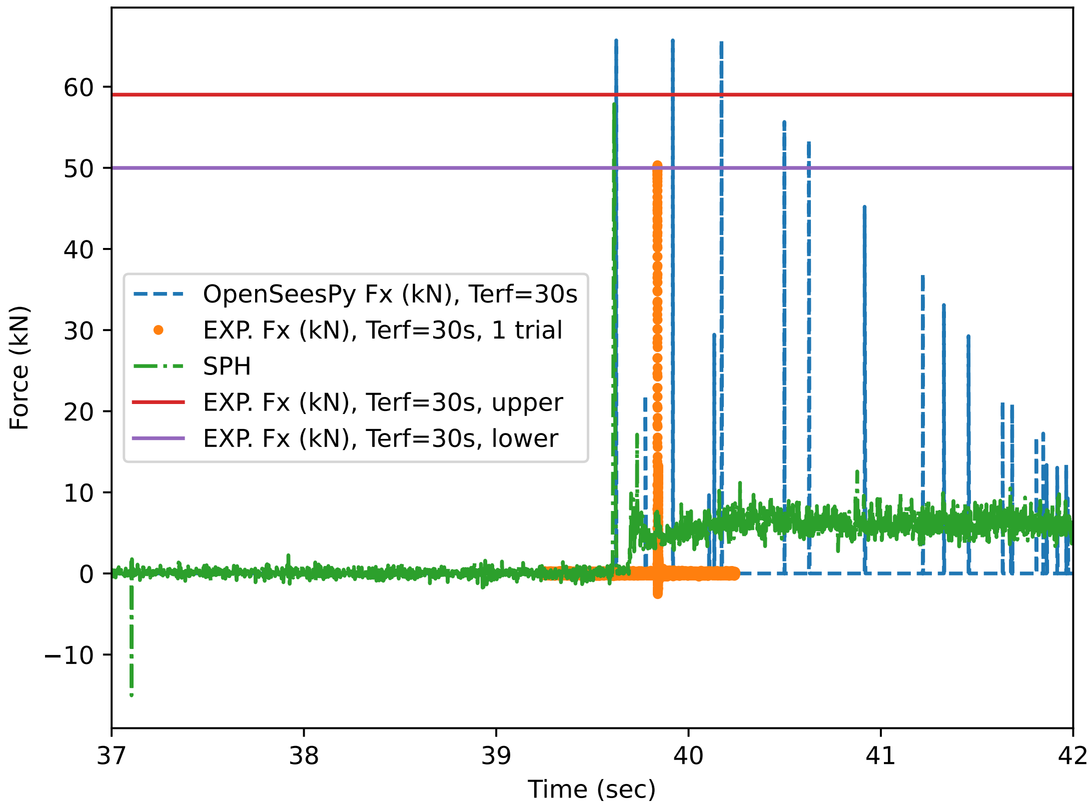

Figure 2.9: Comparison of impact forces between PFEM OpenSeesPy experimental data, and SPH.

2.3.3 Mesh Sensitivity and Run-time

The results shown in Figs. 2.8 and 2.9 are for a PFEM background mesh size of h=0.04 m. The average runtime for this mesh size (2D analysis) is 3.1×10^{-5} seconds per element per iteration per time step with one core for FEM part computation of PFEM and 2.6×10^{-6} seconds per particle per time step with four cores for particles part computation of PFEM. The total runtime is 17 hours for FEM part computation with 143,874 fluid elements and 72 debris elements, and 7.7 hours for particle part computation with 1,518,361 fluid particles.

To assess the sensitivity of the results to mesh size, the simulations are repeated with a larger mesh of h=0.05 m. As shown in Figs. 2.10 and 2.11, the coarser mesh (h=0.05 m) gives generally good results but the wave arrival time and the impact time are delayed by about 0.3 sec. As the mesh size increases, the system becomes stiffer and the fluid moves with a smaller velocity. The average runtime for this mesh size (2D analysis) is 1.6×10^{-5} seconds per element per iteration per time step with one core for FEM computation of PFEM and 2.7×10^{-6} seconds per particle per time step with four cores for particles computation of PFEM. The total runtime is 5.7 hours for FEM part computation with 91,663 fluid elements and 72 debris elements, and 5.1 hours for particle part computation with 971,254 fluid particles.

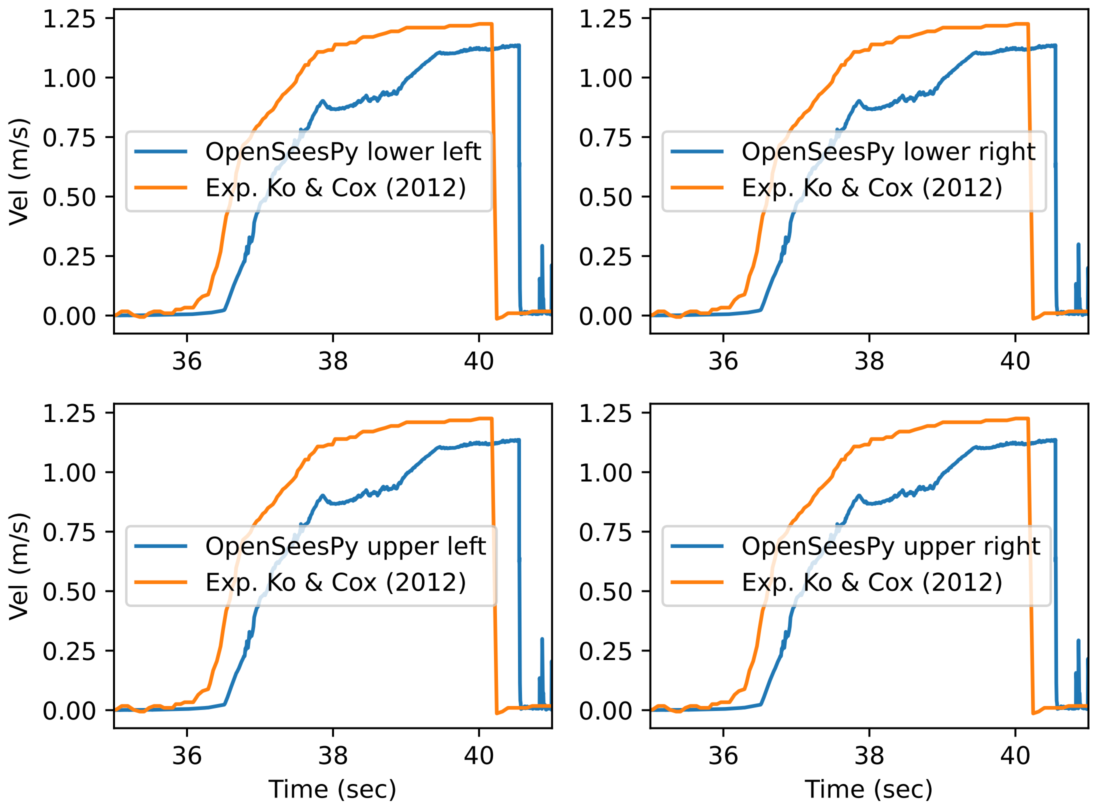

Figure 2.10: The comparison of debris velocities for h=0.05 m.

2.4 ADDITIONAL LESSONS LEARNED FROM PFEM SIMULATIONS

This section details additional modeling considerations and implementation details, above and beyond the modeling issues previously described, e.g., fixing debris rotations and "turning off" FSI for the column in 2D simulations. These items will help other researches avoid similar pitfalls when performing PFEM analyses with OpenSeesPy.

- The contact element for debris and structure impact was implemented with a small frictional damping force which leads to large momentum for the debris in the opposite directions of its movement. By comparing with experimental results, after impact, the debris stays close to the column and has subsequent smaller impacts. The implementation of the contact element was improved with larger frictional damping and the results are greatly improved.

- In PFEM, the number of fluid particles are not associated with the mesh size or the number of fluid elements. This gives flexibility for choosing particles based on the specific problems, and the number of particles becomes problem dependent. In modeling the whole flume analysis as this experiment, experience shows that the number of particles can be related to the number of cells of the background mesh. A cell is a square in 2D or a cube in 3D with its length as the mesh size for the background mesh.

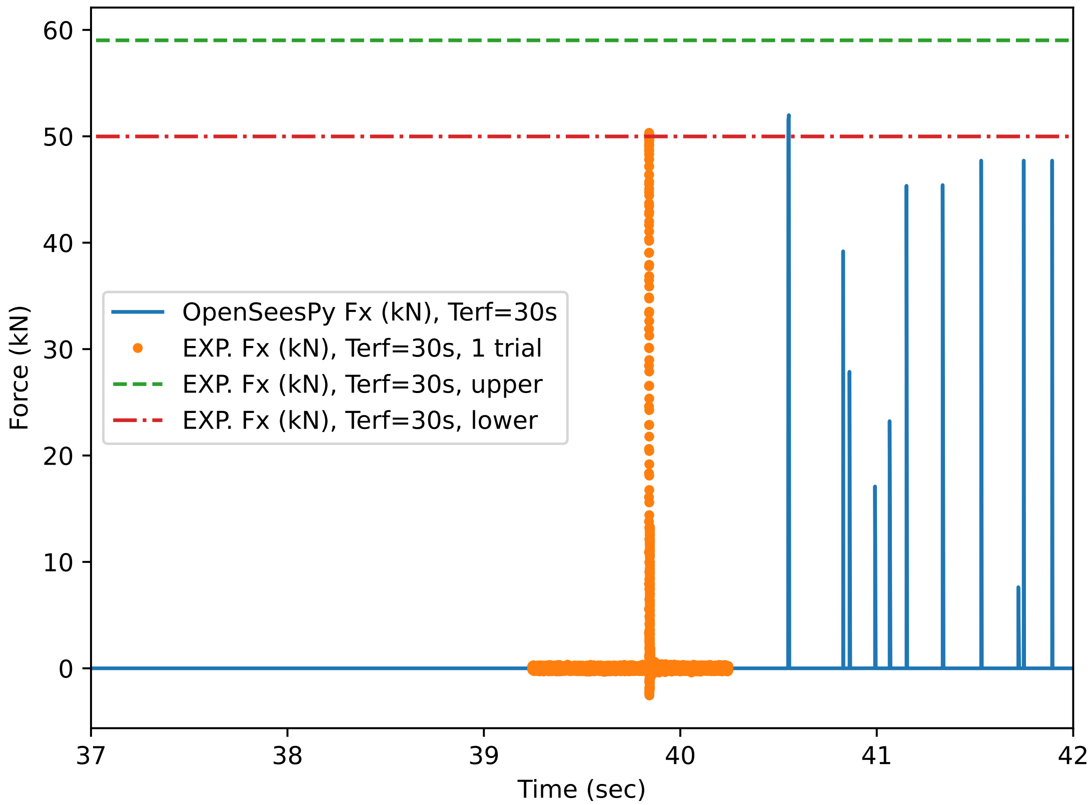

Figure 2.11: The comparison of impact forces for h = 0.05 m.

A starting point is to select the number of particles in each dimension for each cell. Assuming three particles in each dimension, for 2D, it is 9 particles each cell, and 27 particles each cell for 3D problems. Usually, the number of particles in each dimension is between 3 and 4 for problems with wave generations. For dam break problems, this number is suggested to be between 2 and 3. These values are only advisory. The researchers should experiment with different values for their specific problems. Fewer particles run efficiently for the analysis but may reduce the wave amplitude and lose wave energy but too many particles might also overestimate the wave volume and exhaust significant computing resources.

3 Initial 3D Implementation and Testing

While the 2D debris modeling capabilities were fully implemented in OpenSees at the start of this project, the 3D capabilities were still under development. As the project progressed, more 3D debris capabilities were added, particularly a 3D contact element in OpenSees. This chapter presents preliminary results of 3D debris modeling with the PFEM in OpenSeesPy.

3.1 SIMPLE TEST CASE

A simple 3D test case with 4252 debris elements, 180 contact elements, and 38308 fluid elements, was developed to match the 2D debris-fluid-structure interaction model shown in the previous chapter in Fig. 2.7 and the impact force shown in Fig. 2.9.

Since the 3D contact element is not fully tested and a full flume 3D PFEM analysis *with debris* is time consuming in OpenSeesPy, currently only the moment of impact is modeled to test the 3D contact and interaction as shown in Fig. 3.1. The debris model (green) is moving to the left with a prescribed impact velocity and interacting with a fixed column through a layer of 3D contact elements (yellow). This simple example serves as a good starting point to test the 3D contact element formation between the debris and the column through the background mesh, and to test the impact forces generated by the contact elements.

As shown in Fig. 3.2 for the same model with the background mesh turned on, the contact interface can be found quickly in the background grids between the debris and the column, which is fixed and not visible in the figure above. The contact elements are created at the gap between the two solids with the same mesh size of the background mesh.

Two cases are tested for the 3D model with impact velocity v_I=0.85 m/s and v_I=0.9 m/s, and standing water depth 0.3 m. As shown in Fig. 3.3, the impact duration is as short as 2 ms for the experiment and 4 ms for the numerical results. Considering the measuring tolerance, the 3D results give good prediction for the impact duration. A maximum impact force is calculated based on the initial velocity and the stiffness of debris and capped during the impact leading to the horizontal line of the numerical results, which also match the peak impact forces found in the experiment. The results show that the newly developed 3D contact mesh and elements can represent the interaction between the debris and the structure. However, due to the rectangular pulse-like response shown in Fig. 3.3, the dynamic formulation of the 3D contact element requires further investigation.

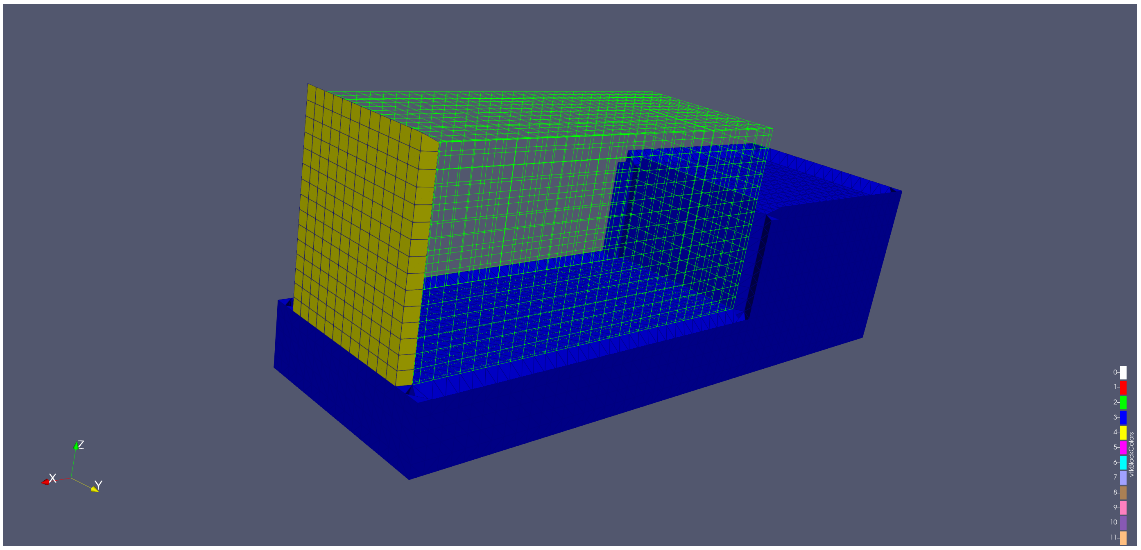

Figure 3.1: The 3D interaction between column and debris. (Yellow - contact elements; Green - debris elements; Blue - fluid elements)

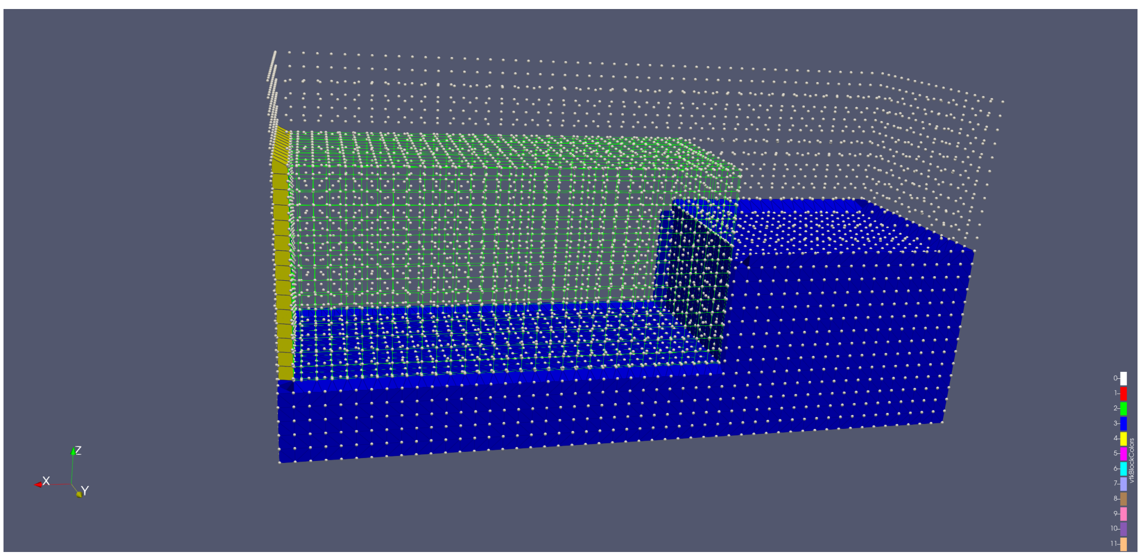

Figure 3.2: The 3D interaction between column and debris with the background mesh turned on. (Yellow - contact elements; Green - debris elements; Blue - fluid elements)

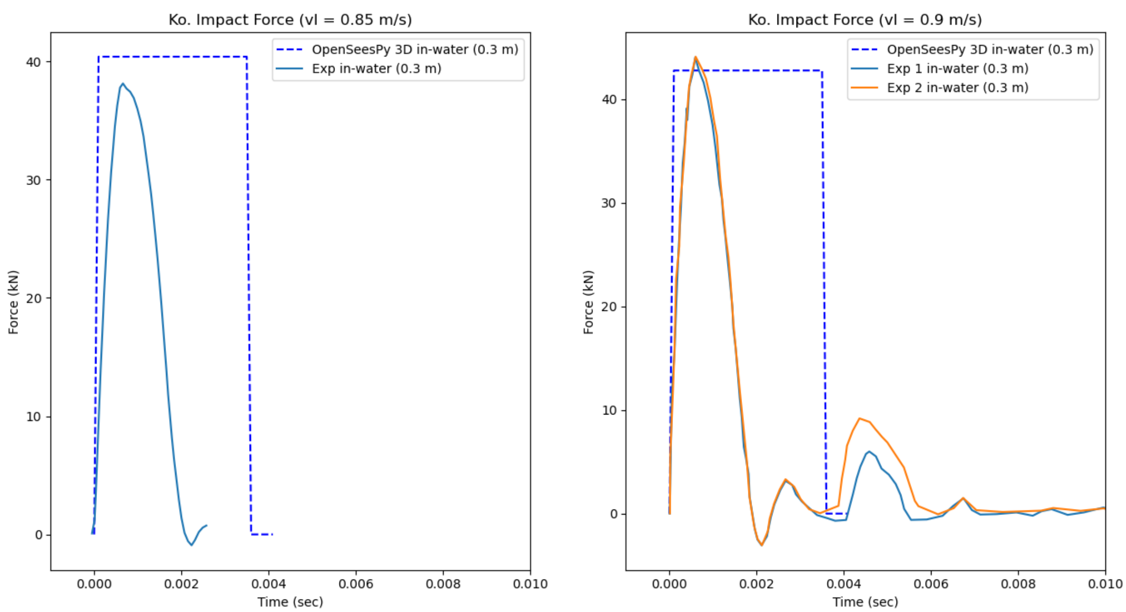

Figure 3.3: The 3D impact forces compared with experiments.

3.2 WAVE ONLY FULL FLUME ANALYSIS

To further test the 3D fluid analysis in preparation for future 3D debris studies using the PFEM in OpenSees, a 3D wave only analysis is performed for the OSU large wave flume. The analysis involves the full flume and the motion of a gate which is lifted in the experiment for generating the waves as described in Shafiei et al. (2016).

The full flume model is shown in Fig. 3.4, where a gate is holding the water tank on the left. A column is placed downstream in the flume. Since the wave only analysis is performed, no debris model is implemented.

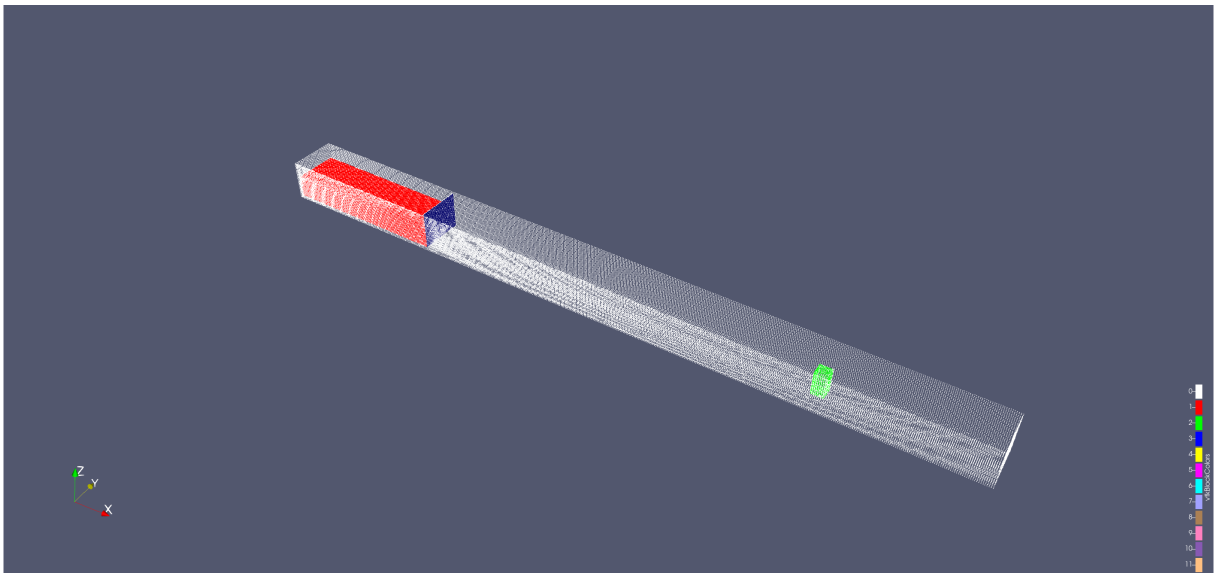

Figure 3.4: The 3D wave only analysis with full flume.

The motion of the gate and the wave propagation in the first few seconds are shown in Fig. 3.5 (a)-(d), which simulates the gate lifting process of the experiment.

Once the wave reaches the column, a normal 3D fluid-structure interaction can be seen in Fig. 3.6 and the fluid is able to move freely around the column. Recall that for 2D analysis, the FSI had to be "turned off" for the column, so that water could continue to flow instead of damming behind the column.

The average runtime for the 3D analysis is 1.9×10^{-5} seconds per time step per element for FEM computations of PFEM with one core and 1.22×10^{-5} seconds per time step per particle for particle computations of PFEM with four cores. Using this metric of time per step per element, the FEM 3D computation appears to be faster than 2D because there are more boundary elements for 3D. Because the boundary elements have fixed displacements and their state determination is trivial, the run time per element reduces.

This simple example shows the capability of the 3D background mesh and that fluid elements are able to interact with 3D structural models for a full flume simulation. Further development is needed to involve the 3D debris models and contact elements in OpenSeesPy PFEM analyses.

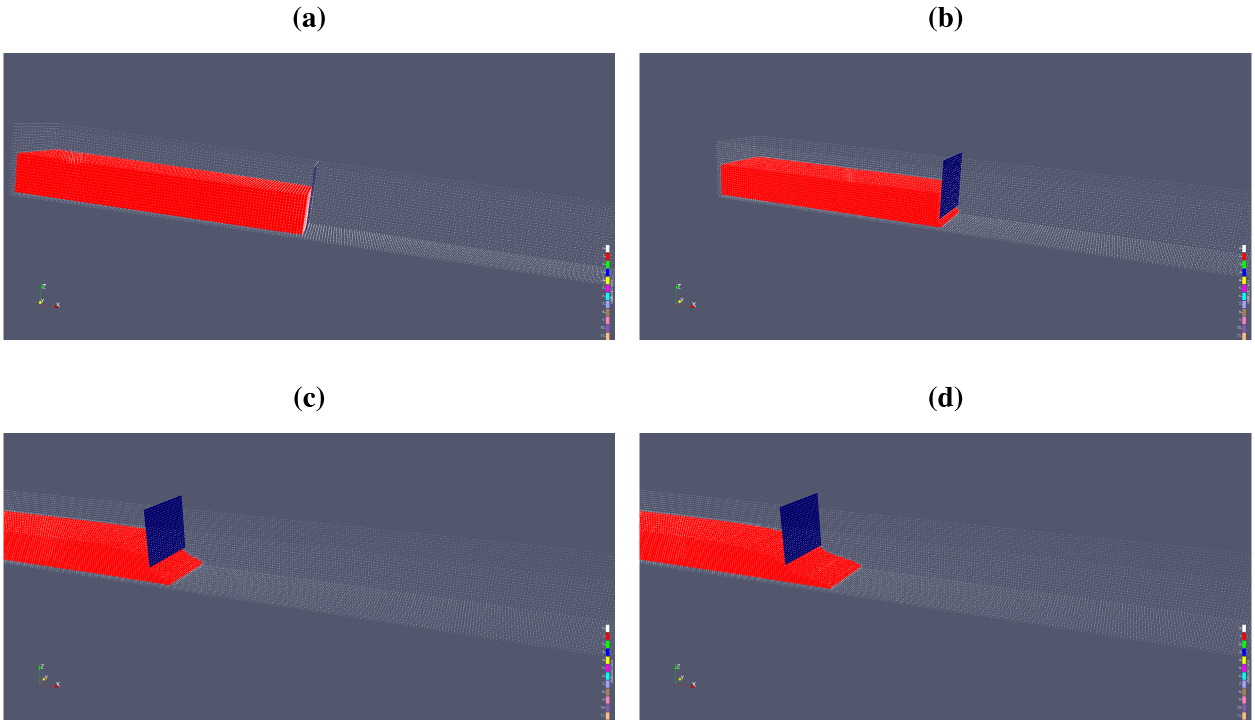

Figure 3.5: The gate lifting and wave propagation.

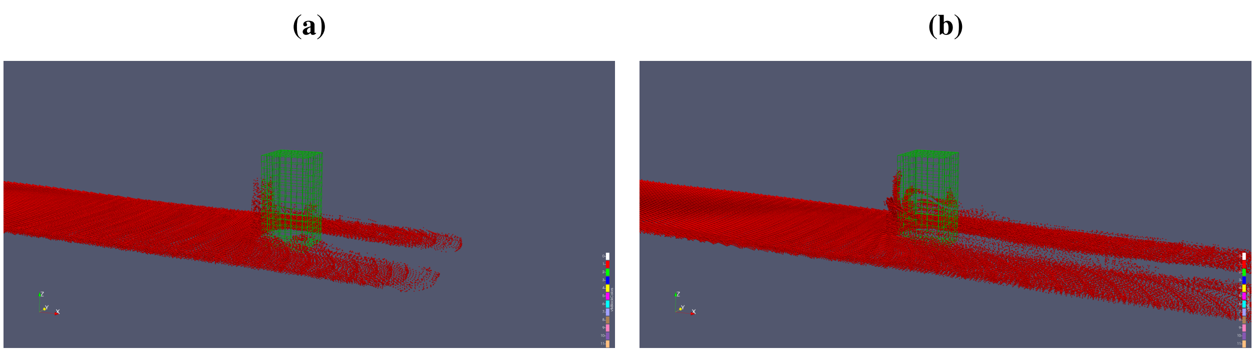

Figure 3.6: The 3D fluid-structure interaction between the wave and the column.

4 Modeling Recommendations and Future Work

To model the flow-driven debris impact on structures, the following recommendations are made based on the analysis of this work.

- The debris is defined as normal nodes and elements. Therefore, the mass of debris can be modeled as either element or nodal mass.
- Damping effects for the structural elements can be modeled using standard approaches, e.g., Rayleigh or modal damping for dynamic response that precedes fluid flow. Additional viscous damping is inherent once the fluid and structure domains interact.
- Since the debris has large displacements, in OpenSeesPy, co-rotational geometric transformation can be used to describe the large displacement and possibly large deformation, e.g., to model crushing of the debris.
- To simulate 3D effect in 2D analysis, for example, fluid can flow around a column, the FSI for single structure in OpenSeesPy can be turned off. The user can decide which structure to interact with the fluid.
- The contact element implemented in OpenSeesPy simulates line-to-line contact between debris and structures, which is generally more accurate than point-to-line and point-to-point contact.

For future work, the three-dimensional debris model and contact model will be extended to support full flume analysis for 3D debris-fluid-structure interaction. Various 3D shapes for debris will also be implemented for quick model building. Further investigation of the 3D contact element response and its accuracy compared to point-based contact formulations will be made.

REFERENCES

Aghl, P.P., Naito, C.J., Riggs, H.R., 2014. Full-scale experimental study of impact demands resulting from high mass, low velocity debris. Journal of Structural Engineering 140. doi:10.1061/(ASCE)ST.1943-541X.0000948.

ASCE, 2022. Minimum Design Loads and Associated Criteria for Buildings and Other Structures. ASCE/SEI 7-16 ed., American Society of Civil Engineers.

Becker, P., Idelsohn, S., Oñate, E., 2015. A unified monolithic approach for multi-fluid flows and fluid–structure interaction using the particle finite element method with fixed mesh. Computational Mechanics 55, 1091–1104. doi:10.1007/s00466-014-1107-0.

Charvet, I., Suppasri, A., Imamura, F., 2014. Empirical fragility analysis of building damage caused by the 2011 great east japan tsunami in ishinomaki city using ordinal regression, and influence of key geographical features. Stochastic Environmental Research and Risk Assessment 28, 1853–1867. doi:10.1007/s00477-014-0850-2.

Como, A., Mahmoud, H., 2013. Numerical evaluation of tsunami debris impact loading on wooden structural walls. Engineering Structures 56, 1249 – 1261. doi:10.1016/j.engstruct.2013.06.023.

Goseberg, N., Heunecke, M., Stolle, J., Nistor, I., 2017. Numerical modelling of shipping container transport over a horizontal bottom, in: International Short Course and Conference on Applied Coastal Research, pp. 3–6.

Haehnel, R., Daly, S., 2004. Maximum impact force of woody debris on floodplain structures. Journal of Hydraulic Engineering 130. doi:10.1061/(ASCE)0733-9429(2004)130:2(112).

Hasanpour, A., 2023. Numerical investigation of tsunami-borne debris interaction with coastal bridges. Ph.D. thesis. University of Nevada Reno. Reno, Nevada.

Hasanpour, A., Istrati, D., Buckle, I., 2021. Coupled SPH-FEM modeling of tsunami-borne large debris flow and impact on coastal structures. Journal of Marine Science and Engineering 10, 1068. doi:10.3390/jmse9101068.

Hasanpour, A., Istrati, D., Buckle, I., 2022. Multi-physics modeling of tsunami debris impact on bridge decks, in: 3rd International Conference on Natural Hazards & Infrastructure, pp. 1–16.

Hasanpour, A., Istrati, D., Buckle, I., (in press). Debris-tsunami-structure interaction and associated loads on coastal bridges. Technical Report 2024/xx. Pacific Earthquake Engineering Research Center, University of California, Berkeley, CA.

Ko, H., D. T. Cox, H. R. Riggs, C. J. Naito, 2015. Hydraulic experiments on impact forces from tsunami-driven debris. Journal of Waterway, Port, Coastal, and Ocean Engineering 141. doi:10.1061/(ASCE)WW.1943-5460.0000286.

Lynett, P.L., Thio, H.K., Scott, M.H., Murphy, T., Shantz, T., Shen, J.D., 2021. Validation of Tsunami Design Guidelines for Coastal Bridges. Technical Report FHWA-OR-RD-21-09. Oregon Department of Transportation. Salem, OR.

McKenna, F., Scott, M.H., Fenves, G.L., 2010. Nonlinear finite-element analysis software architecture using object composition. Journal of Computing in Civil Engineering 24, 95–107. doi:10.1061/(ASCE)ST.1943-541X.0000948.

Nistor, I., Goseberg, N., Stolle, J., 2017. Tsunami-driven debris motion and loads: A critical review. Frontiers in Built Environment 3, 2. doi:10.3389/fbuil.2017.00002.

Oñate, E., Idelsohn, S., Celigueta, M., Rossi, R., Marti, J., Carbonell, J., Ryzhakov, P., Suárez, B., 2011. Advances in the Particle Finite Element Method (PFEM) for Solving Coupled Problems in Engineering. Springer Netherlands. chapter 1. pp. 1–49.

Paczkowski, K., Riggs, H., Naito, C., Lehmann, A., 2012. A one-dimensional model for impact forces resulting from high mass, low velocity debris. Structural Engineering & Mechanics 42, 831–847. doi:DOI:10.12989/sem.2012.42.6.831.

Riggs, H.R., Cox, D.T., Naito, C.J., Kobayashi, M.H., Aghl, P.P., Ko, H.T.S., Khowitar, E., 2013. Water-driven debris impact forces on structures: Experimental and theoretical program, in: International Conference on Offshore Mechanics and Arctic Engineering, Volume 1: Offshore Technology, p. V001T01A059. doi:doi:10.1115/OMAE2013-11128.

Rossetto, T., Peiris, N., Pomonis, A., Wilkinson, S., Del Re, D., Koo, R., Gallocher, S., 2007. The indian ocean tsunami of december 26, 2004: Observations in sri lanka and thailand. Natural Hazards 42. doi:10.1007/s11069-006-9064-3.

Shafiei, S., Melville, B.W., Shamseldin, A.Y., 2016. Experimental investigation of tsunami bore impact force and pressure on a square prism. Coastal Engineering 110, 1–16. doi:10.1016/j.coastaleng.2015.12.006.

Simo, J.C., Hughes, T.J.R., 1998. Computational Inelasticity. Springer-Verlag, New York, NY.

Stolle, J., Nistor, I., Goseberg, N., Petriu, E., 2020. Multiple debris impact loads in extreme hydrodynamic conditions. Journal of Waterway, Port, Coastal and Ocean Engineering 146. doi:10.1061/(ASCE)WW.1943-5460.0000546.

Yeh, H., Barbosa, A.R., Ko, H., Cawley, J.G., 2014. Tsunami loadings on structures: Review and analysis. Coastal Engineering Proceedings 1, 4. URL: https://journals.tdl.org/icce/index.php/icce/article/view/7955, doi:10.9753/icce.v34.currents.4.

Zhu, M., McKenna, F., Scott, M., 2018. OpenSeesPy: Python library for the OpenSees finite element framework. SoftwareX 7, 6–11. doi:10.1016/j.softx.2017.10.009.

Zhu, M., Scott, M.H., 2014. Improved fractional step method for simulating fluid-structure interaction using the PFEM. International Journal for Numerical Methods in Engineering 99, 925–944. doi:10.1002/nme.4727.

Zhu, M., Scott, M.H., 2022. A PFEM Background Mesh for Simulating Fluid and Frame Structure Interaction. Journal of Structural Engineering 148, 04022051. doi:10.1061/(ASCE)ST.1943-541X.00033.

The Pacific Earthquake Engineering Research Center (PEER) is a multi-institutional research and education center with headquarters at the University of California, Berkeley. Investigators from over 20 universities, several consulting companies, and researchers at various state and federal government agencies contribute to research programs focused on performance-based earthquake engineering.

These research programs aim to identify and reduce the risks from major earthquakes to life safety and to the economy by including research in a wide variety of disciplines including structural and geotechnical engineering, geology/seismology, lifelines, transportation, architecture, economics, risk management, and public policy.

PEER is supported by federal, state, local, and regional agencies, together with industry partners.

PEER Core Institutions

University of California, Berkeley (Lead Institution)
California Institute of Technology
Oregon State University
Stanford University
University of California, Davis
University of California, Irvine
University of California, Los Angeles
University of California, San Diego
University of Nevada, Reno
University of Southern California
University of Washington

Pacific Earthquake Engineering Research Center
University of California, Berkeley
325 Davis Hall, Mail Code 1792
Berkeley, CA 94720-1792
Tel: 510-642-3437
Email: peer_center@berkeley.edu

ISSN 2770-8314
https://doi.org/10.55461/GSFH8371